LETTERS

Cretaceous oceanic anoxic event 2 triggered by a massive magmatic episode

Steven C. Turgeon[1] & Robert A. Creaser[1]

Oceanic anoxic events (OAEs) were episodes of widespread marine anoxia during which large amounts of organic carbon were buried on the ocean floor under oxygen-deficient bottom waters[1,2]. OAE2, occurring at the Cenomanian/Turonian boundary (about 93.5 Myr ago)[3], is the most widespread and best defined OAE of the mid-Cretaceous. Although the enhanced burial of organic matter can be explained either through increased primary productivity or enhanced preservation scenarios[1,2], the actual trigger mechanism, corresponding closely to the onset of these episodes of increased carbon sequestration, has not been clearly identified. It has been postulated that large-scale magmatic activity initially triggered OAE2 (refs 4, 5), but a direct proxy of magmatism preserved in the sedimentary record coinciding closely with the onset of OAE2 has not yet been found. Here we report seawater osmium isotope ratios in organic-rich sediments from two distant sites. We find that at both study sites the marine osmium isotope record changes abruptly just at or before the onset of OAE2. Using a simple two-component mixing equation, we calculate that over 97 per cent of the total osmium content in contemporaneous seawater at both sites is magmatic in origin, a ~30–50-fold increase relative to pre-OAE conditions. Furthermore, the magmatic osmium isotope signal appears slightly before the OAE2—as indicated by carbon isotope ratios—suggesting a time-lag of up to ~23 kyr between magmatism and the onset of significant organic carbon burial, which may reflect the reaction time of the global ocean system. Our marine osmium isotope data are indicative of a widespread magmatic pulse at the onset of OAE2, which may have triggered the subsequent deposition of large amounts of organic matter.

OAE2, occurring at the Cenomanian/Turonian boundary (~93.5 Myr ago)[3], is one of several Mesozoic intervals of widespread ocean anoxia[1,2]. OAE2 resulted in a worldwide deposition of organic-rich (black) shales and is demonstrated by an abrupt positive $^{13}C/^{12}C$ ($\delta^{13}C$) excursion[6] in bulk organic matter (up to 6‰) and carbonates (2–3‰)[7]. This isotopic shift, which can be correlated at several distant sites[7], is widely thought to have resulted from an increase in sedimentary burial of ^{13}C-depleted organic carbon in response to the anoxic conditions[8]. In addition to a selective extinction most severely affecting deep-sea benthic foraminifera[9], this episode of carbon sequestration seems to have led to an ephemeral but significant decrease[6] in the partial pressure of atmospheric CO_2 and cooling of surface temperatures[8,10], making this interval of particular interest for studies of the effects of climate change.

It has often been proposed that an important magmatic event such as the emplacement of large igneous provinces (LIPs) or mid-ocean ridges may have triggered OAE2 (refs 4, 5). Although a general consensus on a causal link to the deposition of black shale has yet to be achieved, several feedback scenarios have been proposed. Increased magmatism, for example, in addition to emitting large quantities of CO_2 to the atmosphere, would also have depleted dissolved oxygen through reactions with trace metals and sulphides in hydrothermal fluids[5], thereby increasing the preservation of organic matter on the sea floor. Other feedback mechanisms involve enhancing primary productivity in the oceans either through the release of reduced compounds and biologically limiting elements (for example, iron from a hydrothermal-derived plume[4]), or through increased nutrient flux owing to high sea levels engendered by increased seafloor spreading or remineralization of organic matter in the water column[5,11].

If flood basalt eruption did indeed have a causative role in triggering OAE2, then a major magmatic episode should be coeval with, or should immediately precede, the carbon isotope excursion. However, the linking of magmatism to OAE initiation has relied either on indirect evidence provided by the coincidence of LIP emplacement (such as the Caribbean–Colombian igneous province[12], the Kerguelen and Ontong Java plateaux or the Madagascar flood basalts[13,14]) and trace metals in black shales[12], or on $^{87}Sr/^{86}Sr$ isotopes in the sedimentary record that document the interplay of weathering versus mantle-derived strontium input to the oceans[15]. However, although the strontium isotope record of carbonate sediments close to the Cenomanian/Turonian boundary trends towards less radiogenic values that are indicative of a relative increase in magmatic and hydrothermal input of strontium to the oceans[15], the long residence times of strontium in oceans (~3 Myr) does not allow precise correlation of magmatism to the onset of OAE2. In addition, lead, which has an oceanic residence time of only a few decades, shows a shift in isotopic ratios near the base of OAE2 towards values of Caribbean–Colombian igneous plateau and Madagascar flood basalts[16], two of the largest of the $\sim 20 \times 10^6\,km^3$ of intraoceanic, plume-related basalts erupted near the Cenomanian/Turonian boundary[17].

For this study, $^{187}Os/^{188}Os$ isotopic analyses were performed on two black-shale intervals, ~5,500 km apart during the OAE2: from Demerara rise adjacent to the east-northeast coast of South America (Ocean Drilling Project (ODP) Site 1260B), located in the southern proto-North Atlantic during the Cenomanian–Turonian, as well as from the Furlo section in central Italy, formerly located in the western Tethys seaway. The laminated sediments of Site 1260B consist of a mixture of terrigenous detrital material and carbonates, along with large amounts of organic matter (up to 23 wt%). The $^{13}C/^{12}C$ isotope excursion at this site begins at 426.38 m composite depth (mcd), and the entire OAE2 here is ~1.2 m thick[10] (Fig. 1a). The Furlo section contains several tens of metres of biosiliceous limestones of the Scaglia Bianca Formation, with a ~1-m-thick interval of shales rich in radiolarians and organic carbon (C_{org}; up to 16 wt%) of the Livello Bonarelli, representing the sedimentary expression of OAE2 (ref. 7). In addition, several minor C_{org}-rich intervals ('black levels') are interbedded within the Scaglia Bianca up to ~20 m beneath the Bonarelli. Although the $^{13}C/^{12}C$ isotope record here is discontinuous, the excursion seems to increase suddenly close to the base of the Livello Bonarelli (Fig. 1b)[11].

[1]Department of Earth and Atmospheric Sciences, University of Alberta, Edmonton, Alberta, T2G 2E3, Canada.

©2008 Macmillan Publishers Limited. All rights reserved

Most of the osmium in black shales is derived from seawater, with the $^{187}Os/^{188}Os$ ratio being representative of contemporaneous seawater[18]. The isotopic composition of dissolved osmium in modern oceans is nearly homogeneous, with a present-day ratio of ~1.06 (ref. 18). This ratio reflects mass balance between osmium input from hydrothermal alteration of juvenile oceanic crust ($^{187}Os/^{188}Os = 0.127$), average riverine input from continental weathering ($^{187}Os/^{188}Os = 1.4$), together with a generally minor extraterrestrial contribution from meteorites and cosmic dust particles ($^{187}Os/^{188}Os = 0.127$) to the global ocean[19]. The short oceanic residence time of osmium (~10,000 yr; ref. 18) allows short-term (thousands of years) fluctuations in seawater isotopic composition to be precisely recorded in sediments.

At both study sites, the marine $^{187}Os/^{188}Os$ record changes abruptly just at or before the $\delta^{13}C_{org}$ excursion of ~3‰ (refs 10, 11) defining the OAE2 onset (Fig. 1; see Supplementary Data). At Site 1260B, osmium isotope values decrease irregularly from 0.69–1.0 to 0.54 before OAE2, and decrease to 0.17 a few centimetres before the OAE. These very low osmium isotope values persist through OAE2 to ~426.0 mcd before gradually increasing further up the section, and return to ~0.6 a few decimetres above OAE2. At Furlo, osmium isotope values in the black levels show a slight decline (from 0.92 to 0.66) beneath the Bonarelli, suggesting that the relative fluxes of the major osmium inputs to oceans remained somewhat steady before the onset of OAE2, perhaps over timescales of 1–3 Myr (ref. 20). An abrupt decrease in marine $^{187}Os/^{188}Os$ from 0.66 to 0.16 occurs between the uppermost black level and the base (comprising roughly the lower one-third) of the Bonarelli. The osmium isotope values then gradually increase further up the section, returning to 0.46. The marine osmium isotope and $\delta^{13}C_{org}$ records are antithetic through the OAE2 at both sites. The $^{187}Os/^{188}Os$ values at the base of OAE2 are similar to the isotopic shift reported for OAE1a (ref. 21), suggesting similar control mechanisms for at least some of the other Cretaceous OAEs. Before OAE2 (up to ~426.5 mcd at Site 1260B and pre-Bonarelli at Furlo), osmium contents are low (<1 ng g^{-1}) but increase abruptly just before the OAE at Site 1260B and close to the base of the Bonarelli at Furlo to >14 ng g^{-1}. In addition, an apparent double spike of osmium enrichment occurs at both sites in the interval of low $^{187}Os/^{188}Os$ ratios (Fig. 1). The similar structure and magnitude of osmium records (contents and isotopic ratios) at both sites strongly suggest that these signals are primary in nature, and that the same process(es) were operating at both sites.

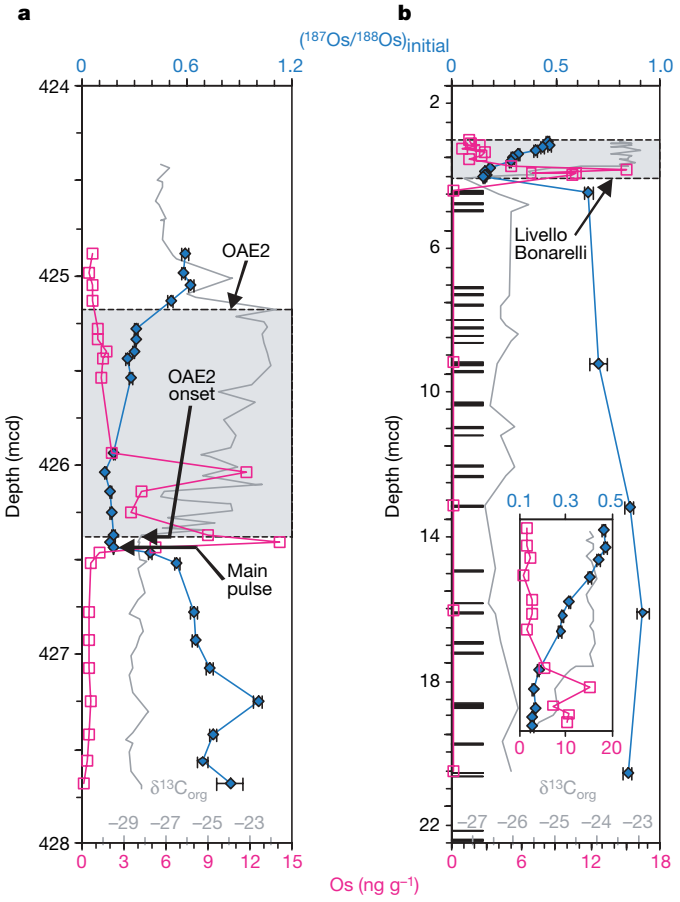

Figure 1 | Initial seawater $^{187}Os/^{188}Os$ isotope ratios (blue), Os contents (red), and $\delta^{13}C_{org}$ values (grey) for the two studied sites. **a**, ODP207 Site 1260B ($n = 25$); **b**, Furlo, Italy ($n = 17$). The extent of the OAE for Site 1260B is based on carbon isotope ratios. Horizontal black bars represent location of black levels beneath the Bonarelli at Furlo. The inset shows data points within the Livello Bonarelli. Error bars represent 2σ uncertainties of calculated initial seawater osmium isotope ratios. $\delta^{13}C_{org}$ values are from ref. 10 for Site 1260B and from ref. 11 for Furlo.

Using a simple two-component mixing equation assuming chondritic (0.127) and bulk continental (1.4) osmium isotopic end-members[18], we calculate that over 97% of the total osmium content at both sites is magmatic in origin (in comparison with ~27% for present-day oceans). This represents a ~30–50-fold increase relative to pre-OAE conditions, assuming a constant riverine input. Furthermore, the osmium contents at the base of the OAE2 interval for both sites show enrichment factors of the same order of magnitude as under pre-OAE2 conditions, suggesting that the increased osmium contents mainly reflect a change in the seawater osmium inventory. Osmium isotope data have also been used as a marker of onset of volcanic activity just before the Triassic/Jurassic boundary in the Central Atlantic magmatic province[22] and the Cretaceous/Tertiary boundary in the Deccan flood basalts[23].

Although the low $^{187}Os/^{188}Os$ values at the OAE might also result from an extraterrestrial source, such as the impact of a large bolide[19], iridium profiles within the Bonarelli at Furlo[24] do not support this hypothesis, and typical impact-related features such as shocked quartz have not been reported from OAE2. The apparently prolonged (on the order of 190 kyr at Site 1260B, estimated from the duration data of ref. 10) input of mantle-derived osmium with a low $^{187}Os/^{188}Os$ ratio to the oceans is also consistent with existing data showing an increase in several trace elements, including zinc—which is commonly associated with hydrothermal activity[19]—at both Furlo and at Site 1260B (S.C.T., unpublished observations). Our osmium content records at both sites, in conjunction with a marine residence time of osmium in the modern ocean of ~10 kyr (ref. 18), indicate a high, but variable, input of osmium to the oceans—probably from at least two major magmatic pulses—during the early phases of OAE2. The specific pathway(s) for transfer of unradiogenic osmium from LIP magmatism to the oceans is poorly constrained, but conceivably involves the seafloor hydrothermal processes invoked for fluxes of other metals at OAE2 (see, for example, ref. 4). However, the osmium contents of both high-temperature and low-temperature hydrothermal fluids from mid-ocean-ridge settings are generally close to, or below, concentrations in sea water[25]. This observation suggests that the release of unradiogenic osmium during LIP emplacement—as indicated by our isotopic data—probably occurred at much higher flux rates and/or fluid concentrations than is typical of known mid-ocean ridge hydrothermal systems.

The difference in timing between the onset of magmatism, demonstrated by the sharp decrease in seawater $^{187}Os/^{188}Os$, and the carbon isotope excursion (Fig. 1) can be estimated by assuming a constant sediment accumulation rate—a reasonable tenet given that no major trends are observed in lithogenic proxies (for example, titanium, aluminium and rubidium) at either site (ref. 20, and S.C.T., unpublished observations). Consistent with previous work, we use a duration of 550 kyr for the OAE2 $\delta^{13}C$ excursion, a value in the upper range of proposed durations (ref. 10), and derive an accumulation rate of ~218 cm Myr^{-1} for OAE2 at Site 1260B. The maximum calculated time-lag between the osmium and $\delta^{13}C$ records is ~23 kyr;

©2008 Macmillan Publishers Limited. All rights reserved

using an OAE2 duration of only 220 kyr (ref. 26)—a value in the lower range of published duration estimates—the time-lag would be ~9 kyr.

Although the exact mechanism responsible for this time-lag is unclear, at Site 1260B a prominent organic-rich layer (426.43–426.38 mcd)—syndepositional with the onset of low osmium ratios—implies an immediate response of the oceans to magmatism, at least at the regional scale. The later shift of $\delta^{13}C$ values defining OAE2 onset, however, suggests a feedback mechanism possibly involving a carbon burial 'threshold'. A similar trend is recorded by sea surface temperatures (ref. 10), which, although seeming to shift before the $\delta^{13}C$ excursion, increase only after the onset of magmatism. On this basis, we suggest that the time-lag between osmium and C isotope records resulted from initial buffering of the effects of magmatism by a stratified ocean. It has long been proposed that Cenomanian–Turonian oceans were stratified and characterized by low turnover rates and sluggish circulation[27]. At Site 1260, nanofossils indicative of ocean stratification and a deep nutricline are in decline at the beginning of OAE2, whereas indicators of primary productivity increase only after the $\delta^{13}C$ shift[28]. Thus, the initial increase in carbon burial at the onset of OAE2 might have resulted solely from an increased preservation of organic matter related to magmatism-induced bottom-water anoxia. A subsequent breakdown in stratification would have increased surface-water fertility through the shallowing and/or upwelling of nutrient- and biologically limiting element-rich bottom waters, enhancing primary productivity. A scenario of upward expansion of reducing bottom waters during OAE2 is consistent with the observed sequential extinction of benthic foraminifera and, subsequently, intermediate-water foraminifera[29].

It has long been postulated that large-scale magmatic activity initially triggered the Cenomanian–Turonian OAE, but a direct proxy of magmatism preserved in the sedimentary record, coinciding closely to the onset of OAE2, has not yet been found. The marine osmium isotope record clearly shows that a widespread magmatic pulse occurred just at or before the onset of OAE2 at the Cenomanian/Turonian boundary and probably triggered the subsequent deposition of large amounts of organic matter preserved in the OAE2 interval.

METHODS SUMMARY

Sediment and a mixed rhenium–osmium spike were digested with a CrO_3–H_2SO_4 solution in sealed tubes. The osmium was then separated with chloroform and subsequently reacted with hydrobromic acid (HBr). The chloroform was then removed and the osmium-bearing HBr was evaporated. The residue was microdistilled twice with a chromium solution to volatilize osmium, and was collected in HBr. Final dry-down of the HBr was performed under a nitrogen atmosphere. An aliquot of the rhenium-bearing CrO_3–H_2SO_4 solution, diluted in water, was reduced by bubbling with SO_2 cleaned through water in a gas-washing bottle. The rhenium was purified by using anion chromatography. Analytes were then loaded onto nickel (for rhenium) and platinum (for osmium) filaments, and analysed by isotope dilution–thermal ionization mass spectrometry in negative-ion mode. Isotopic ratios were corrected for instrumental mass fractionation, isobaric oxygen interferences, spike and blank contributions. Errors for isotope ratios were determined by numerical error propagation and include uncertainties in spike calibration, weighing, and analytical/instrumental measurements, as well as rhenium bias, oxygen, and blank corrections.

Initial seawater osmium isotopes were determined from

$$(^{187}Os/^{188}Os)_{initial} = (^{187}Os/^{188}Os)_{measured} - (^{187}Re/^{188}Os)_{measured} \times (e^{\lambda t} - 1)$$

where λ is the ^{187}Re decay constant ($\lambda^{187}Re$) of $1.666 \times 10^{-11}\,yr^{-1}$ and t is the age of the sedimentary rock. The relative mass balance equation used to estimate the contribution of mantle-derived osmium to seawater is $R_{sw} = xR_{mtl} + yR_{chon} + zR_{cont}$, where R denotes $^{187}Os/^{188}Os$ ratios and the subscript sw represents the calculated initial seawater value, and mtl, chon and cont denote mantle, chondritic and continental sources, respectively. The factors x, y and z are the relative contributions of each source. Extraterrestrial contributions are assumed to be negligible[19]. The relative contribution of mantle-derived osmium can therefore be estimated by using $x = (R_{cont} - R_{sw})/(R_{cont} - R_{mtl})$. Values for R_{cont} and R_{mtl} are 1.4 and 0.127, respectively[18].

Full Methods and any associated references are available in the online version of the paper at www.nature.com/nature.

Received 3 October 2007; accepted 1 May 2008.

1. Schlanger, S. O. & Jenkyns, H. C. Cretaceous anoxic events: causes and consequences. *Geol. Mijnb.* **55,** 179–184 (1976).
2. Schlanger, S. O., Arthur, M. A., Jenkyns, H. C. & Scholle, P. A. The Cenomanian–Turonian Oceanic Anoxic Event, I. Stratigraphy and distribution of organic carbon-rich beds and the marine $\delta^{13}C$ excursion. *Spec. Publ. Geol. Soc. (Lond.)* **26,** 371–399 (1987).
3. Gradstein, F. M. *et al. A Geologic Time Scale* (Cambridge Univ. Press, Cambridge, 2004).
4. Sinton, C. W. & Duncan, R. A. Potential links between ocean plateau volcanism and global ocean anoxia at the Cenomanian–Turonian boundary. *Econ. Geol.* **92,** 836–842 (1997).
5. Kerr, A. C. Oceanic plateau formation: a cause of mass extinction and black shale deposition around the Cenomanian–Turonian boundary. *J. Geol. Soc. Lond.* **155,** 619–626 (1998).
6. Kuypers, M. M. M., Pancost, R. D. & Sinninghe Damsté, J. S. A large and abrupt fall in atmospheric CO_2 concentration during Cretaceous times. *Nature* **399,** 342–345 (1999).
7. Tsikos, H. *et al.* Carbon-isotope stratigraphy recorded by the Cenomanian–Turonian Oceanic Anoxic Event: correlation and implications based on three key localities. *J. Geol. Soc. Lond.* **161,** 711–719 (2004).
8. Arthur, M. A., Dean, W. E. & Pratt, L. M. Geochemical and climatic effects of increased marine organic carbon burial at the Cenomanian/Turonian boundary. *Nature* **335,** 714–717 (1988).
9. Kaiho, K. & Hasegawa, T. End-Cenomanian benthic foraminiferal extinctions and oceanic dysoxic events in the northwestern Pacific Ocean. *Palaeogeogr. Palaeoclimatol. Palaeoecol.* **111,** 29–43 (1994).
10. Forster, A., Schouten, S., Moriya, K., Wilson, P. A. & Sinninghe Damsté, J. S. Tropical warming and intermittent cooling during the Cenomanian/Turonian oceanic anoxic event 2: Sea surface temperature records from the equatorial Atlantic. *Paleoceanography* **22,** doi:10.1029/2006PA001349 (2007).
11. Jenkyns, H. C., Matthews, A., Tsikos, H. & Erel, Y. Nitrate reduction, sulfate reduction, and sedimentary iron isotope evolution during the Cenomanian–Turonian oceanic anoxic event. *Paleoceanography* **22,** doi:10.1029/2006PA001355 (2007).
12. Snow, L. J., Duncan, R. A. & Bralower, T. J. Trace element abundances in the Rock Canyon Anticline, Pueblo, Colorado, marine sedimentary section and their relationship to Caribbean plateau construction and oxygen anoxic event 2. *Paleoceanography* **20,** doi:10.1029/2004PA001093 (2005).
13. Storey, M. *et al.* Timing of hot-spot related volcanism and the breakup of Madagascar and India. *Science* **267,** 852–855 (1995).
14. Torsvik, T. H. *et al.* Late Cretaceous magmatism in Madagascar: palaeomagnetic evidence for a stationary Marion hotspot. *Earth Planet. Sci. Lett.* **164,** 221–232 (1998).
15. McArthur, J. M., Kennedy, W. J., Chen, M., Thirlwall, M. F. & Gale, A. S. Strontium isotope stratigraphy for Late Cretaceous time: Direct numerical calibration of the Sr isotope curve based on the US Western Interior. *Palaeogeogr. Palaeoclimatol. Palaeoecol.* **108,** 95–119 (1994).
16. Kuroda, J. *et al.* Contemporaneous massive subaerial volcanism and late cretaceous Oceanic Anoxic Event 2. *Earth Planet. Sci. Lett.* **256,** 211–223 (2007).
17. Wignall, P. B. Large igneous provinces and mass extinctions. *Earth Sci. Rev.* **53,** 1–33 (2001).
18. Peucker-Ehrenbrink, B. & Ravizza, G. The marine osmium isotope record. *Terra Nova* **12,** 205–219 (2000).
19. Pegram, W. J. & Turekian, K. K. The osmium isotopic composition change of Cenozoic sea water as inferred from a deep-sea core corrected for meteoritic contributions. *Geochim. Cosmochim. Acta* **63,** 4053–4058 (1999).
20. Turgeon, S. & Brumsack, H.-J. Anoxic vs dysoxic events reflected in sediment geochemistry during the Cenomanian–Turonian Boundary Event (Cretaceous) in the Umbria–Marche Basin of central Italy. *Chem. Geol.* **234,** 321–339 (2006).
21. Suzuki, K. *et al.* Secular change of Early Cretaceous seawater Os isotope composition: an indicator of a LIP-OAE link (abstract). *Japan Geoscience Union Meeting, 19–24 May 2007*, <www.jpgu.org/publication/cd-rom/2007cd-rom/program/pdf/C104/C104-013_e.pdf> (2007).
22. Cohen, A. S. & Coe, A. L. New geochemical evidence for the onset of volcanism in the Central Atlantic magmatic province and environmental change at the Triassic–Jurassic boundary. *Geology* **30,** 267–270 (2002).
23. Ravizza, G. & Peucker-Ehrenbrink, B. Chemostratigraphic evidence of Deccan volcanism from the marine osmium isotope record. *Science* **302,** 1392–1395 (2003).
24. Alvarez, W., Alvarez, L. W., Asaro, F. & Michel, H. V. The end of the Cretaceous: Sharp boundary or gradual transition? *Science* **223,** 1183–1186 (1984).
25. Sharma, M., Rosenberg, E. J. & Butterfield, D. A. Search for the proverbial mantle osmium sources to the oceans: Hydrothermal alteration of mid-ocean ridge basalt. *Geochim. Cosmochim. Acta* **71,** 4655–4667 (2007).

©2008 Macmillan Publishers Limited. All rights reserved

26. Lamolda, M. A., Gorostidi, A. & Paul, C. R. C. Quantitative estimates of calcareous nannofossil changes across the Plenus Marls (latest Cenomanian), Dover, England: implications for the generation of the Cenomanian–Turonian Boundary Event. *Cretac. Res.* **15,** 143–164 (1994).
27. Barron, E. J. A. Warm, equable Cretaceous: The nature of the problem. *Earth Sci. Rev.* **19,** 305–338 (1983).
28. Hardas, P. & Mutterlose, J. Calcareous nannofossil assemblages of Oceanic Anoxic Event 2 in the equatorial Atlantic: Evidence of an eutrophication event. *Mar. Micropaleontol.* **66,** 52–69 (2007).
29. Jarvis, I. *et al.* Microfossil assemblages and the Cenomanian–Turonian (late Cretaceous) Oceanic Anoxic Event. *Cretac. Res.* **9,** 3–103 (1988).
30. Selby, D. & Creaser, R. A. Re–Os geochronology of organic rich sediments: An evaluation of organic matter analysis methods. *Chem. Geol.* **200,** 225–240 (2003).

Supplementary Information is linked to the online version of the paper at www.nature.com/nature.

Acknowledgements We thank E. Erba for support, D. Tiraboschi for sampling assistance, A. Vogel and K. Jones for help in sample preparation, B. Kendall for discussions and suggestions, and J. Hallowes and G. Hatchard for technical assistance. Site 1260B samples were provided by the Integrated Ocean Drilling Program. This study was supported by a Natural Science and Engineering Research Council (NSERC) Discovery Grant. The Radiogenic Isotope Facility at the University of Alberta is supported in part by an NSERC Major Resources Support Grant.

Author Information Reprints and permissions information is available at www.nature.com/reprints. Correspondence and requests for materials should be addressed to S.C.T. (turgeonsc@ualberta.ca).

©2008 Macmillan Publishers Limited. All rights reserved

METHODS

Sample preparation. Large (over ~30 g) samples were powdered with non-metallic methods to avoid potential contamination by osmium-bearing metallic particles. Powdered sediment (0.5 g), representing a 1–2-cm thickness, and a mixed ^{185}Re–^{190}Os spike were digested for 48 h at 80 °C in sealed Carius tubes with a $Cr^{VI}O_3$–H_2SO_4 solution. All analyses were performed at the Radiogenic Isotope Facility of the Department of Earth and Atmospheric Sciences, University of Alberta, and are modified from ref. 30.

Osmium separation. After digestion, the osmium was separated and purified by solvent extraction three times with 3.5 ml of chloroform added to 3 ml of 9 M HBr and heated overnight to 80 °C. The chloroform was then removed and the HBr was evaporated at 80 °C. The residue was microdistilled with 30 μl of Cr solution (0.2 g of CrO_3 per ml of 3 M H_2SO_4) collected in 20 μl of 9 M HBr inside a conical Savillex vial and heated to 80 °C for 3 h. The HBr is then dried and redistilled. Final dry-down of the osmium-bearing HBr was performed at 50 °C under a nitrogen atmosphere.

Rhenium chromatography. A 1-ml aliquot of the rhenium-bearing CrO_3–H_2SO_4 solution was diluted with 1 ml of 18.2 MΩ cm water and the Cr^{VI} reduced to Cr^{III} by bubbling for ~15–30 s with SO_2 cleaned through water in a gas-washing bottle. Anion chromatography was then performed on disposable polyethylene columns with Eichrom 1-X8 100–200-mesh anion resin. The sample solution was loaded on the column and washed with 4 ml of 1.0 M HCl, 1 ml of 0.2 M HNO_3 and 1.5 ml of 6 M HNO_3, and rhenium was eluted with 4 ml of 6 M HNO_3, collected in a clean beaker and evaporated to dryness. The residue was dissolved in 200 μl of 0.05 M HNO_3, and further purified with a single DOWEX AG1-X8 <20-mesh anion bead. The 0.05 M HNO_3 was discarded and replaced with 1 ml of 6 M HNO_3 overnight, and evaporated to dryness at 80 °C.

Mass spectrometry. Purified analytes were loaded onto nickel (for rhenium) and platinum (for osmium) filaments, and isotopic compositions were measured with isotope dilution–thermal ionization mass spectrometry on a VG Sector 54 instrument in negative-ion mode. Isotopic ratios were corrected for instrumental mass fractionation by using $^{185}Re/^{187}Re = 0.59738$ and $^{192}Os/^{188}Os = 3.08261$, isobaric oxygen interferences, spike and blank contributions. Total procedural blanks were <15 and <0.5 pg for rhenium and osmium, respectively, with a $^{187}Os/^{188}Os$ blank ratio of ~0.20. In-house standard solutions were analysed repeatedly to monitor long-term mass spectrometer reproducibility. Errors for isotope ratios were determined by numerical error propagation and include uncertainties in spike calibration, weighing, and analytical/instrumental measurements, as well as rhenium bias, oxygen and blank corrections.

Initial seawater osmium isotope calculations. Initial seawater osmium isotopes were determined from

$$(^{187}Os/^{188}Os)_{initial} = (^{187}Os/^{188}Os)_{measured} - (^{187}Re/^{188}Os)_{measured} \times (e^{\lambda t} - 1)$$

where λ is the ^{187}Re decay constant ($\lambda^{187}Re$) of 1.666×10^{-11} year^{-1} and t is the age of the sedimentary rock (93.5 Myr). No adjustments were made for the duration of the OAE2; even with a higher estimate of 0.55 Myr in duration (ref. 10), the initial osmium isotopes would vary by <0.4% on average.

Mass balance calculations. The relative mass balance equation used to estimate the contribution of mantle-derived osmium to seawater is $R_{sw} = xR_{mtl} + yR_{chon} + zR_{cont}$, where R denotes $^{187}Os/^{188}Os$ ratios and the subscript sw represents the calculated initial seawater value, and mtl, chon and cont denote mantle, chondritic and continental sources, respectively. The factors x, y and z are the relative contributions of each source. Extraterrestrial contributions are assumed here to be negligible[19] and constant for this period, and therefore the relative contribution of mantle-derived osmium can then be estimated by using $x = (R_{cont} - R_{sw})/(R_{cont} - R_{mtl})$. Values for R_{cont} and R_{mtl} are 1.4 and 0.127, respectively[18].

©2008 Macmillan Publishers Limited. All rights reserved